Phonon and elastic instabilities in rocksalt alkali hydrides under pressure: First-principles study

Jingyun Zhang,[1] Lijun Zhang,[1] Tian Cui,[1] Yan Li,[1] Zhi He,[1] Yanming Ma,[1,2,*] and Guangtian Zou[1]
[1]*National Lab of Superhard Materials, Jilin University, Changchun 130012, People's Republic of China*
[2]*Laboratory of Crystallography, Department of Materials, ETH Zurich, Wolfgang-Pauli-Strasse 10, CH-8093 Zurich, Switzerland*
(Received 18 September 2006; revised manuscript received 14 December 2006; published 26 March 2007)

The lattice and elastic instabilities of rocksalt (RS) alkali hydrides (LiH, NaH, KH, RbH, and CsH) under pressure are extensively studied to reveal the physically driven mechanism of the phase transition from RS to CsCl structure by using the pseudopotential plane-wave method within density functional theory. A universal pressure-induced soft transverse acoustic (TA) phonon mode is identified at the zone boundary X point in the Brillouin zone for these compounds, signifying a structural instability. A predicted charge transfer from alkali to hydrogen with pressure might be attributable to the phonon softening. Moreover, a softening behavior in C_{44} shear modulus with pressure is predicted for NaH, KH, RbH, and CsH, while it is absent for LiH. Analysis of the calculated results suggested that with increasing pressure the predicted TA phonon softening behaviors, instead of C_{44} shear modulus instability, is mainly responsible for the pressure-induced structural phase transition. Furthermore, the current phonon calculations suggest that there might exist a similar RS $\rightarrow$ CsCl phase transition in LiH.

DOI: 10.1103/PhysRevB.75.104115 PACS number(s): 64.70.Kb, 62.50.+p, 63.20.Dj

The properties of materials under high pressure and temperature have attracted much attention because of their relevance for understanding the compositions of the Earth's interior and other planetary interiors. Accurate first-principles methods can complement and help to interpret high-pressure experiments, which can provide a detailed description of the structural and bonding changes that a material undergoes under extreme conditions. The behavior of hydrogen at high pressure is central to a number of fundamental problems in condensed matter and planetary science.[1] The possibility of the formation of the proton hydride at high pressure has recently been raised.[2] Moreover, the metal-hydrogen systems have received wide attention partly due to the large number of technical applications.[3] Among the different classes of hydrogen compounds, the alkali hydrides (LiH, NaH, KH, RbH, and CsH) form "so-called" ionic hydrides. Support for this view can be obtained from the observed crystal structures of rocksalt (RS) and CsCl for these compounds which are typical for ionic systems.[4]

It is known that the alkali hydrides crystallize with the RS structure at ambient pressure.[5] Except for LiH, under high pressure, NaH, KH, RbH, and CsH were observed to transform to CsCl structure at pressures of 29.3,[7] 4.0,[6] 2.2,[6] and 0.83 GPa,[8] respectively. Also, Ghndehari *et al.*[8] observed a further transformation of CsCl to a CrB structure (*Cmcm* space group) at a higher pressure of 17.5 GPa for CsH, while no experimental measurements suggest the existence of such phase transition for NaH, KH, and RbH. On the theoretical side, Kuiljov *et al.*[9] using an empirical equation of states (EOS) firstly predicted a RS $\rightarrow$ CsCl transition in LiH with a transition pressure in the range of 50–100 GPa. Hammerberg *et al.*[10] using a Heine-Abarenkov type pseudopotential with an empty core for Li^+ ion predicted also a RS $\rightarrow$ CsCl transition in LiH at about 200 GPa. Later, Martins *et al.*[11] using *ab inito* pseudopotential method within local density approximation (LDA) calculated the EOS of LiH, NaH, and KH and suggested that the transition in LiH would occur only at very high pressures of 450 to 500 GPa. Recently, Ahuja *et al.*[12] theoretically predicted the similar phase transition sequence of CsCl to CrB for KH and RbH by means of the total-energy calculations within LDA using the full-potential linear muffin-tin orbital (LMTO) method. More recently, Saitta *et al.*[13] successfully demonstrated that the CsCl to CrB phase transition in CsH is attributable to the combination of a shear deformation and an atomic distortion associated with an M_2^- phonon mode.

However, to the best of our knowledge, the physically driven mechanism of the pressure-induced structural phase transition of RS $\rightarrow$ CsCl in NaH, KH, RbH, and CsH is still elusive. Dynamical[14] and elastic instabilities[15] are often responsible for phase transitions under pressure. In our previous works,[16,17] the different mechanisms driving the phase transitions in copper halides are clearly revealed by the accurate *ab initio* determination of the transverse acoustic (TA) phonon softening at the zone boundary X and L point for CuCl and CuI, respectively, and along the $[\xi\xi 0]$ direction for CuBr in the first Brillouin zone (BZ). Moreover, dynamical instabilities are usually attributable to a negative elastic constant for a particular shear mode, which are often related to the martensitic transformation between fcc and bcc structures via the tetragonal Bain's path.[18–21] Therefore, lattice dynamics and elastic behaviors play an important role in understanding the mechanisms of the phase transitions. To probe the physically driven mechanism of the phase transition in the RS alkali hydrides, detailed *ab initio* calculations of the lattice dynamics and elastic constants for these compounds are, thus, motivated.

Pseudopotential plane-wave *ab initio* calculations were performed within the framework of density functional theory.[22] The generalized gradient approximation (GGA) exchange-correlation functional was employed.[23] The norm-conserving scheme is used to generate the pseudopotentials for Li, Na, K, Rb, Cs, and H, respectively. A nonlinear core correction to the exchange-correlation energy functional was introduced to generate pseudopotentials for Li, Na, and Cs. Instead, $3p$ and $4p$ semicore states are incorporated into the valence electrons for K and Rb, respectively. The core radii

TABLE I. Calculated equilibrium lattice parameter (a_0), bulk modulus (B_0), and the pressure derivative of bulk modulus (B_0') for LiH, NaH, KH, RbH, and CsH. Previous theoretical calculations and experimental results are also shown for comparison. The units for a_0 and B_0 are in a.u. and GPa, respectively.

		a_0 (a.u.)	B_0 (GPa)	B_0'
LiH				
	This work	7.44	34.30	3.40
	Ref. 30	7.56	36.60	3.40
	Expt.	7.67[a]	34.24[b]	3.80±0.15[b]
NaH				
	This work	9.02	21.60	3.76
	Ref. 29	8.90	28.00	
	Expt.	9.22[c]	19.40±2.00[c]	4.40±0.50[c]
KH				
	This work	10.77	13.30	3.70
	Ref. 11	11.32	12.00	4.20
	Expt.	10.83[e]	15.6±1.50[e]	4.00±0.50[e]
RbH				
	This work	11.71	11.70	3.47
	Ref. 28	10.90	14.10	
	Expt.	11.43[c]	10.00±1.00[d]	
CsH				
	This work	12.11	9.61	4.52
	Ref. 28	11.20	8.80	
	Expt.	12.07[c]	7.60±0.80[d]	4.00±0.40[d]

[a]Reference 31.
[b]Reference 32.
[c]Reference 7.
[d]Reference 33.
[e]Reference 6.

for H, Li, Na, K, Rb, and Cs are chosen to be sufficiently small to guarantee the core nonoverlapping under compression in this study. Convergence tests gave a kinetic energy cutoff E_{cutoff} as 70 Ry and a $8\times8\times8$ Monkhorst-Pack[24] (MP) grid (k mesh) for the electronic BZ integration. The lattice dynamics of these compounds were investigated by using the linear-response method.[25] A $12\times12\times12$ MP k mesh was found to yield phonon frequencies converged to within 0.05 THz. A $4\times4\times4$ q mesh in the first BZ was used in the interpolation of the force constants for the phonon dispersion curve calculations. The elastic constant tensors were calculated as a function of pressure using the stress-strain relations. Elastic constants were obtained from evaluations of the stress tensor generated by small strains using the density-functional plane wave technique as implemented in the CASTEP code.[26]

The theoretical equilibrium lattice constant is determined by fitting the total energy as a function of volume to the Murnaghan EOS.[27] The calculated equilibrium lattice parameters and bulk modulus, together with other pseudopotential plane-wave theoretical calculations[11,28–30] and the experimental data[6,7,31–33] are listed in Table I. It is clear that the current theoretical lattice constants and bulk modulus are in good agreement with experimental data within 3%. The excellent agreement strongly supports the choice of pseudopotentials and the GGA approximation for the current study. The calculated EOS of LiH, NaH, and KH in rocksalt structure are compared with the experimental data[34,7,10] as shown in Fig. 1. The agreement between theoretical results and the experimental data is also satisfactory, lending another support in the validity of the current theoretical model.

The left panel in Fig. 2 shows the comparison of the calculated phonon dispersion curves with the experimental data (solid squares)[35] for LiH at ambient conditions. With the addition of the nonanalytic term to the dynamical matrix, the longitudinal optic (LO) phonon branch and the transverse optic (TO) phonon branch split from each other at the Γ point, and this is shown. It is clear that the calculated

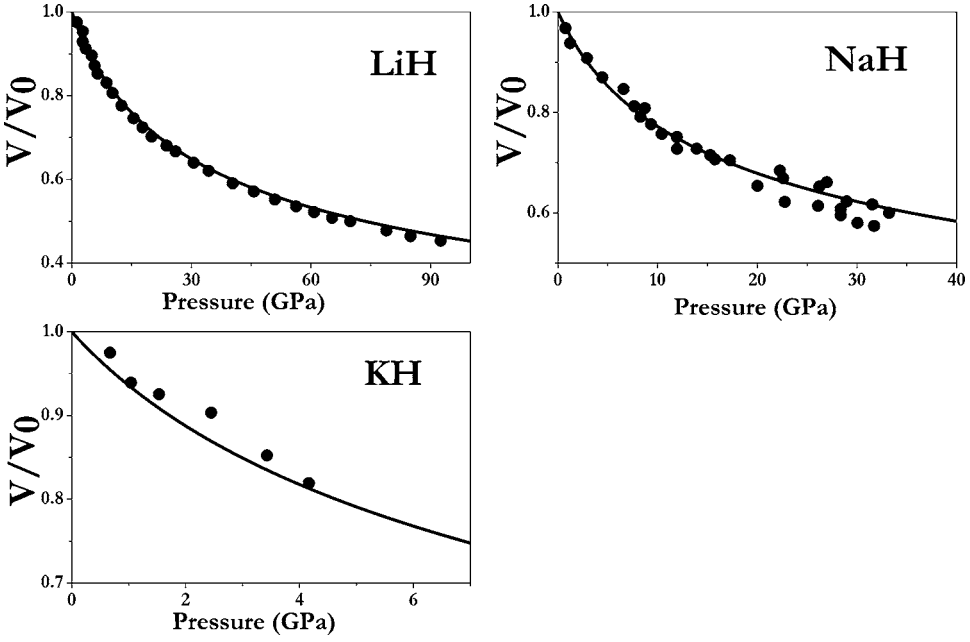

FIG. 1. Comparison of the calculated equation of states (solid line) for LiH, NaH, and KH with the experimental data (solid square symbols) from Refs. 34, 7, and 10, respectively.

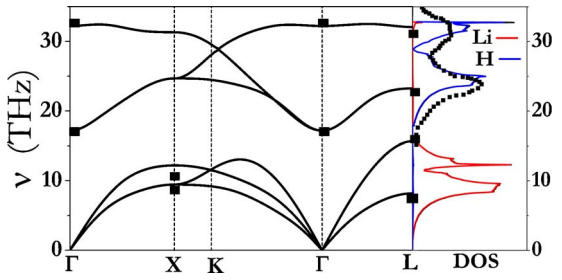

FIG. 2. (Color online) Calculated phonon dispersion curves (left panel) and hydrogen projected phonon density of states (right panel) for LiH together with the experimental data. Solid squares in the left and right panel are the experimental data taken from Refs. 35 and 36, respectively. Solid lines are the calculated results. Blue and red lines are the theoretical hydrogen and lithium projected phonon density of states, respectively.

phonons at several high symmetry points of Γ, X, and L in the BZ are in good agreement with experimental data[35] (deviations ⩽6%). The right panel in Fig. 2 shows the calculated projected phonon density of states (DOS) together with the experimental data of the hydrogen-projected phonon DOS.[36] The hydrogen-projected phonon DOS reads $Z_H(E) = \frac{1}{3N}\Sigma_q\Sigma_{j=1}^{6}|\sigma_H(q,j)|^2\delta[E-E(q,j)]$, where q is a phonon wave vector in the first BZ, N is the number of these wave vectors, j labels the six phonon branches, $\sigma_H(q,j)$ is a polarization vector for H, and $E(q,j)$ is the phonon energy. It is important to note that the H atom mainly contributes to the high frequency vibrations because of its relatively lighter atomic mass, while Li atom dominates the low frequency vibrations as indicated in Fig. 2. One observes that the theoretical hydrogen-projected phonon DOS agrees well with the experimental data. Specifically, two main peak positions are well reproduced in spite of the noticeable discrepancy in the peak width in the high frequency region. Also, it is worth reminding that many difficulties have been found in the past in tackling with alkali hydrides, especially for LiH, because of the extreme reactivity of the samples which can spoil the experimental findings; for example, the infrared spectra are very sensitive to the cleanness of the surface.[37] The good agreement between theoretical calculations and the experimental measurements characterizes the first-principles GGA calculations of this kind and supports the accuracy of both the experimental measurements and the current theoretical model. Figure 3(a)–3(d) represent the comparison of the simulated hydrogen-projected phonon DOS (at theoretical equilibrium volume) with experimental inelastic neutron scattering measurements[38] for NaH, KH, RbH, and CsH, respectively, at ambient pressure. It is significant to note that the agreement between theory and experiment is excellent for NaH, KH, and RbH. For CsH, although the relative distribution and curve shape are well reproduced, the agreement is less satisfied by evidence of a ~1.3 THz frequency higher in the first frequency peak of theoretical calculation. This discrepancy might be mainly attributed to the insufficient TO and LO splitting at zone center in theory and the difference in the equilibrium lattice constant between the current calculation and the experiment data. Nevertheless, the overall good agreement in phonons between theory and experiments in alkali hydrides at zero pressure ensures us to explore the high pressure properties.

We have calculated the complete phonon dispersion curves for LiH, NaH, KH, RbH, and CsH with increasing pressure. However, for simplicity and as a representative, Fig. 4 only presents the calculated phonon dispersion curves for RbH at different volumes. We found that at the theoretical equilibrium volume of the RS structure, all phonon modes are stable. From Fig. 4, it is interesting to note that with decreasing volume, the TO, LO, and longitudinal acoustic (LA) phonon modes shift to higher frequencies, while the TA phonon branch along the [100] direction decreases in

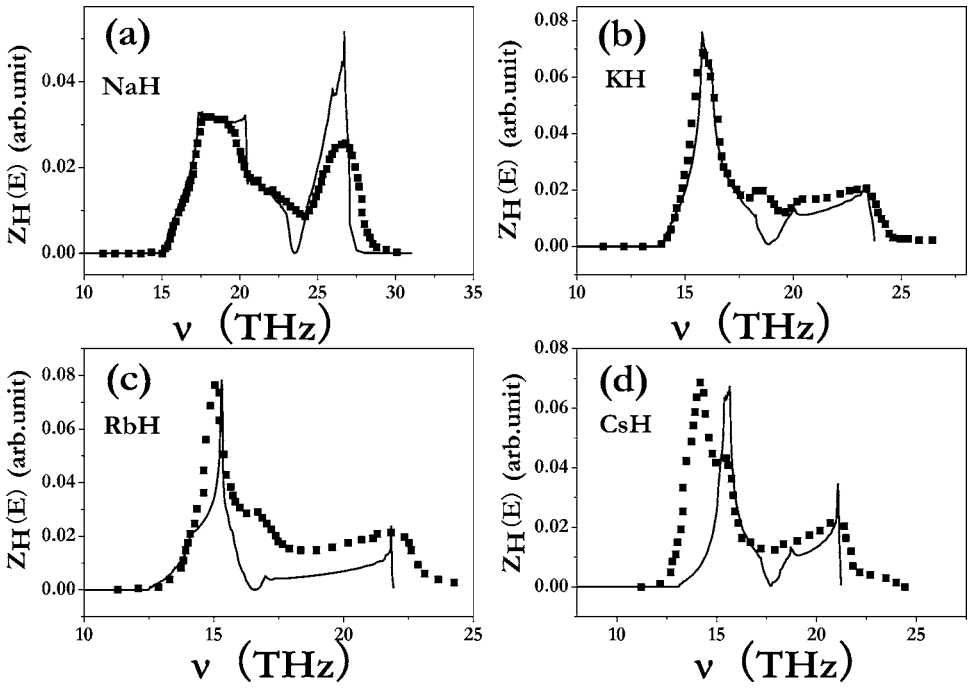

FIG. 3. Comparison between experimental results (Ref. 38) (solid squares) and theoretical hydrogen projected phonon density of states (solid lines) for NaH (a), KH (b), RbH (c), and CsH (d), respectively.

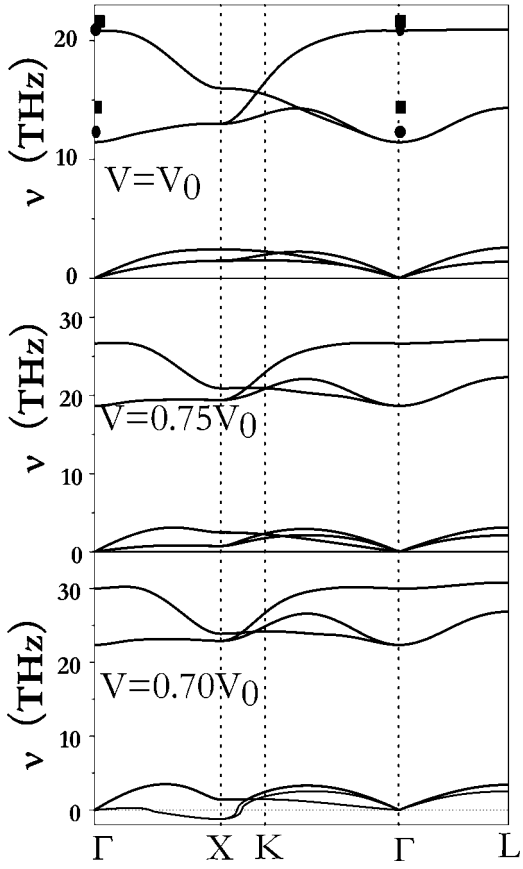

FIG. 4. The calculated phonon dispersion curves of RbH at different volumes. Solid squares and solid circles are the previous calculations taken from Refs. 49 and 38, respectively.

frequency, indicating a negative mode Grüneisen parameter $\gamma_j(q) = -\partial \ln \nu_j(q) / \partial \ln V$ for mode j, where q is wave vector, ν is frequency, and V is volume. It is significant that with an increase in pressure the TA phonon frequency at the zone boundary X (0.0 0.0 1.0) point softens to imaginary frequencies at $V=0.70V_0$ (V_0, theoretical equilibrium volume), indicating a structural instability. Figure 6(c) shows the variation of the frequency of the TA (X) mode with volume. The estimated volume of phonon softening to zero frequency is $0.72V_0$ corresponding to a transition pressure of 7.0 GPa, which is somewhat larger than the experimental transition pressure of ~2.2 GPa.

It is very interesting to note that for LiH, NaH, KH, and CsH a similar TA (X) phonon softening is also predicted. Figures 5(a), 6(a), 6(b), and 6(d) show the variations of TA (X) phonon frequency with volume for LiH, NaH, KH, and CsH, respectively. The estimated volumes for phonon softening to zero frequency for LiH, NaH, KH, and CsH are $\sim 0.37V_0$, $\sim 0.44V_0$, $\sim 0.61V_0$, and $\sim 0.80V_0$ (V_0 is the theoretical equilibrium volume), corresponding to the pressures of ~200, ~90, ~18, and ~3.5 GPa, respectively. It is clear that the predicted transition pressures corresponding to zero phonon frequency for NaH, KH, and CsH are also higher than the experimental transition pressures of 29.3 GPa for NaH, 4.0 GPa for KH, and 0.83 GPa for CsH. The overestimated pressures are ~60.7, 14.0, 4.8, and 2.67 GPa for NaH,

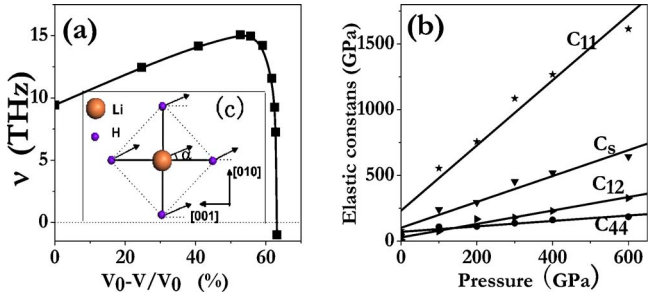

FIG. 5. (Color online) The calculated TA (X) phonon frequency (a) and elastic constants (b) as a function of volume and pressure for LiH, respectively. Solid symbols are the calculated data. Solid line through the calculated data in panel (a) represents fitted curves using a B spline. Solid lines in panel (b) through the calculated data represent a linear fit. (c) the eigenvector for TA soft phonon mode at the X (1.0 0.0 0.0) point for LiH. The Li atom is located at (0, 0, 0). The other four H atoms sit at $(0,1/2,0)$, $(0,-1/2,0)$, $(0,0,1/2)$, and $(0,0,-1/2)$ respectively. The angle α equals to 33.44°. The arrows show the directions of atomic displacements.

KH, RbH, and CsH,[39,50] respectively, showing a decreasing trend with reduced atomic mass of alkali metals. It is noteworthy that the TA (X) phonon frequencies for LiH and NaH with pressure go up first and then turn down to the imaginary values as shown in Figs. 5(a) and 6(a). This intriguing feature postpones the occurrence of phonon instability and results in a much larger theoretical transition pressure in LiH and NaH. A clearly remarkable feature is represented by the strong similarity of the softening trend of TA (X) in the last three alkali hydrides: it suggests that KH, RbH, and CsH could be gathered together in a subgroup of compounds rather different from LiH,[36,40] while NaH being a sort of "crossover" alkali metal hydride, which is usually observed in crystal chemistry.

In general, the predicted universal TA (X) phonon softenings in RS alkali hydrides shed a strong light on the physical mechanism behind the phase transition. The somewhat large difference in transition pressures between theory and experiment indicates that the phase transition from RS to CsCl structure might not be induced independently by the dynamic instability. However, although the phase transition occurs at pressures below those required to drive TA (X) modes to zero frequency, the "mode softening" behavior may be related to the particular mechanisms which is responsible for the phase transition. The RS structured alkali hydrides, therefore, tends to become unstable with respect to the atomic displacement corresponding to the soft mode. Inspection of the phonon eigenvector shows that this mode involves alternate shuffles of (100) planes. Interestingly, in the eigenvector for this soft mode both Li atom and H atoms form the angles of $\alpha = 33.44°$ with respect to the [001] direction, which is shown in the inset of Fig. 5(a). The atomic movements along the directions of the eigenvectors in the (100) planes is closely related to the phase transition from RS to CsCl structure. The eigenvectors for the TA (X) softening phonon modes of NaH, KH, RbH, and CsH are quite similar to that of LiH, except for the difference in the α values. The formed angles α are 8.81°, 85.45°, 2.75°, 27.29° for NaH, KH, RbH, and CsH, respectively.

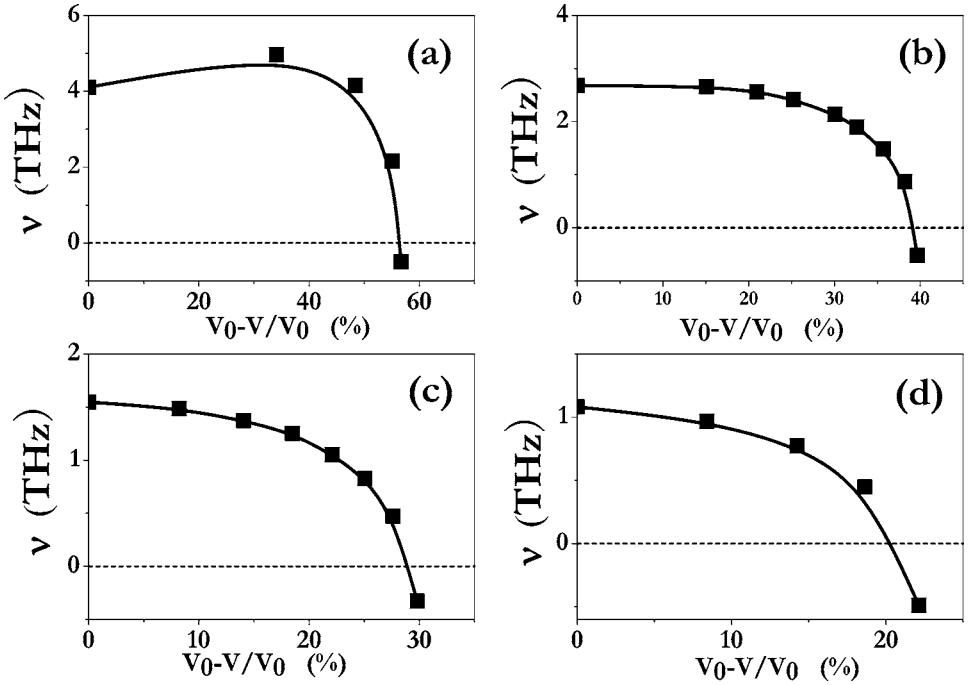

FIG. 6. The calculated TA (X) phonon frequencies in NaH (a), KH (b), RbH (c), and CsH (d) as a function of volume. Solid lines through the calculated data are B-spline fitted curves.

Figure 7(a) presents the partial density of states (PDOS) of NaH at zero pressure. It is clear that most of Na 3s electrons have transferred to Na 3p and H 1s orbitals. The significant charge transfer from Na 3s to H 1s suggests an ionic bonding feature between Na and H. Moreover, the overlapped electron bands of Na 3p and H 1s in the PDOS imply a covalent bonding nature. Therefore, the H-Na bond is a mixture of covalency and ionicity. To further demonstrate the mixed bonding behavior of NaH, we use Mulliken population analysis[41] to explore the bond overlap population (BOP) as shown in Fig. 7(b). The BOP was widely used to assess the covalent or ionic bonding nature of particular bulk crystals.[42] A high value of the BOP indicates a high degree of covalency in the bond, while a low value indicates a more ionic interaction. At zero pressure, the calculated BOP for NaH is 0.64$|e|$, which sits between 0.87$|e|$ of covalent Si and 0.22$|e|$ of ionic NaCl.[42] This fact strongly supports the above electron PDOS results. With increasing pressure, the BOP of NaH was reduced from 0.64$|e|$ at zero pressure to 0.32$|e|$ at 90 GPa as shown in Fig. 7(b), indicating a more ionic bonding feature under high pressure and a pressure-induced charge transfer from Na to H. The variations of Mulliken

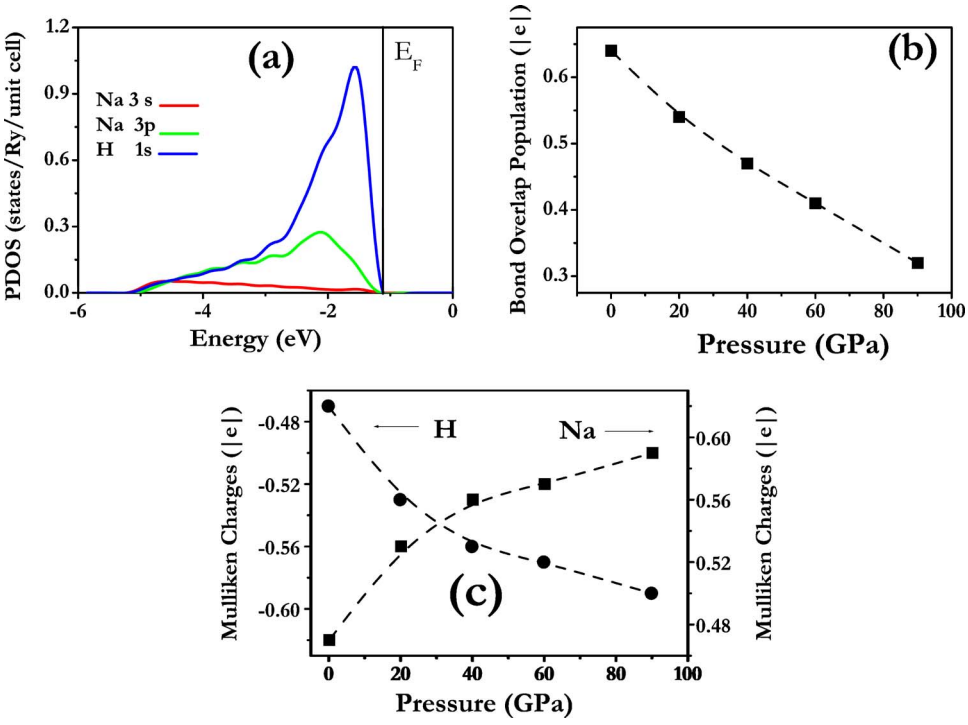

FIG. 7. (Color online) (a) The calculated electron partial density of states for NaH at zero pressure. (b) and (c) are the calculated bond overlap population and Mulliken charges for NaH with pressure, respectively; The symbols are the calculated data and the lines are the guides for the eye. In (c), left scale is for H, while right scale is for Na.

TABLE II. Calculated elastic constants of C_{11}, C_{12}, C_s, and C_{44} for alkali hydrides at ambient pressure. Previous theoretical calculations (Ref. 28) and experimental results are also shown for comparison. For LiH, the available experimental data are taken from Ref. 46.

		C_{11} (GPa)	C_{44} (GPa)	C_{12} (GPa)	C_s (GPa)
LiH					
	This work	82.7	52.5	10.7	36.0
	Expt. 46	66.4	45.8	15.6	25.4
	Ref. 28	99.1	59.8	11.2	44.0
NaH					
	This work	53.2	22.7	14.8	19.2
	Ref. 28	43.8	26.1	19.2	12.3
KH					
	This work	26.8	10.6	6.5	10.2
	Ref. 28	32.8	12.9	8.0	12.4
RbH					
	This work	24.6	8.2	4.6	10.0
	Ref. 28	28.2	12.5	7.2	10.5
CsH					
	This work	22.4	5.8	3.2	9.6
	Ref. 28	20.3	9.1	3.1	8.6

charges with pressure for Na and H are explicitly shown in Fig. 7(c). A pressure-induced charge transfer from Na to H is clearly revealed to support the validity of the BOP calculation. Mulliken population analysis is also performed for other alkali hydrides (not shown). A similar pressure-induced charge transfers from alkali atoms to hydrogen in all alkali hydrides were thus concluded. It is also interesting to note that the alkali hydrides become more ionic under high pressure. The predicted charge transfer might significantly alter the competing attractive and repulsive forces between the nearest neighbors, thereby possibly inducing a soft phonon mode.[43] As mentioned above from the right panel of Fig. 2, the softening TA phonon modes are dominated by the vibration of alkali atoms. This charge depletion induced phonon softening is similar to that in the B-doped diamond in which $C \rightarrow B$ charge transfers drive a Raman redshift.[44,45]

Table II lists the calculated elastic constants for RS alkali hydrides, together with experimental data for LiH[46] and previously theoretical results[28] at ambient pressure. It is found that our calculated elastic constants for LiH, NaH, KH, and CsH at zero pressure are in reasonable agreement with the experimental data[46] and previous theoretical calculations.[28] The variations of the elastic constants with pressure for RS alkali hydrides are shown in Figs. 5(b) and 8. It is clear that C_{11}, C_{12}, and Cs exhibits linearly increasing trends with pressure for all the alkali hydrides. However, C_{44} shows a linear softening trend for NaH, KH, RbH, and CsH. Surprisingly, on the contrary, it is found that C_{44} in LiH increases monotonically as shown in Fig. 4(b). We used both norm-conserving and ultrasoft pseudopotentials together with much larger k mesh in the elastic constant calculation to check the validity of the increasing trend for C_{44} in LiH with pressure. All the evidences supported the correctness of the current calculation. Two points have to be addressed to understand this fact. First, LiH differs from other alkali hydrides, which has higher heat of formation[47] and cohesive energy[48] than other alkali hydrides, indicating a stronger bonding in LiH. Secondly, A higher hydrogen-hydrogen mid-bond charge density in LiH was previously suggested and a decrease in hydrogen-hydrogen density and an increase in anion-cation interaction with alkali masses were predicted.[28] The above two aspects might be closely related to the C_{44} anomaly in LiH. It is noteworthy that although C_{44} softens with pressure for NaH, KH, RbH, and CsH, it still remains positive under pressures at which the phonons soften to zero frequency. It should be also pointed out that for these com-

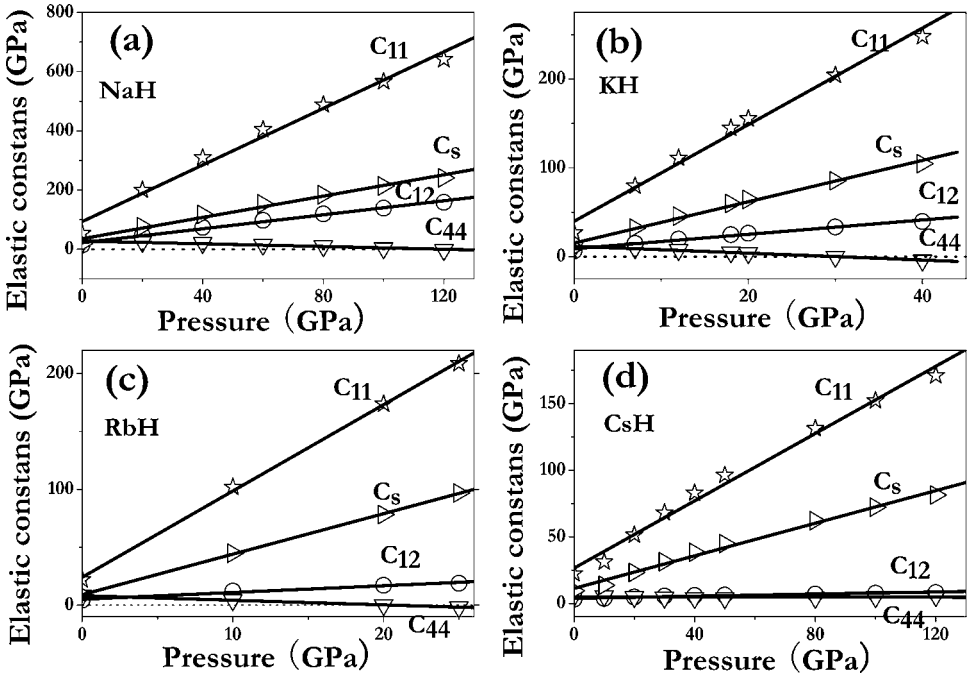

FIG. 8. Calculated elastic constants (solid symbols) of C_{11}, C_{12}, C_s, and C_{44} for NaH (a), KH (b), RbH (c), and CsH (d) with pressure in RS structure. The solid lines are the linear fits to the calculated results.

pounds, the phonon instabilities occur at points away from the center of the BZ and appear before the materials become unstable according to elastic stability criteria. Therefore, it is concluded that the pressure-induced structural phase transition for these compounds is not dominated by the C_{44} instabilities which are related to the long-wavelength part of the transverse branch near the center of the first BZ.

In this work, we have extensively studied the lattice dynamics and elastic constants of RS alkali hydrides under pressure using the *ab initio* pseudopotential plane-wave method. We predicted a universal pressure-induced soft TA phonon mode at the zone boundary X point for these compounds. Moreover, a softening behavior in C_{44} shear modulus with pressure is verified for NaH, KH, RbH, and CsH, while it is absent for LiH. Analysis of the calculated results suggested that with increasing pressure the predicted TA phonon softening behaviors, instead of C_{44} shear modulus instability, is closely related to the pressure-induced structural phase transition from RS to CsCl. From the currently predicted phonon softening behaviors for LiH, One might also expect a similar RS→CsCl phase transition in LiH which did not confirm by experiments yet. The calculated pressure for the TA (X) phonon mode softening to zero frequency in LiH is ~200 GPa as deduced from Fig. 5(a), which is now accessible in the experiment.

We thank Artem R. Oganov for helpful comments on this paper, and the financial support of the China 973 Program under Grant No. 2005CB724400, the NSAF of China under Grant No. 10676011, the National Doctoral Foundation of China Education Ministry under Grant No. 20050183062, the SRF for ROCS, SEM, the Program for 2005 New Century Excellent Talents in University, and the 2006 Project for Scientific and Technical Development of Jilin Province. Most of calculations in this work have been done using the QUANTUM-ESPRESSO package.[51]

*Email address: mym@jlu.edu.cn

[1] H. K. Mao and R. J. Hemley, Am. Sci. **80**, 234 (1992).
[2] B. Baranowski, Pol. J. Chem. **66**, 1737 (1992).
[3] G. G. Libowitz, J. Phys. Chem. Solids **55**, 1461 (1994).
[4] B. Baranowski, M. Tkacz, and S. Marjchrzak, *Pressure Dependence of Hydrogen Volume in Some Metallic Hydrides in Molecular Systems Under High Pressure*, edited by R. Pucci and G. Piccitto (North-Holland, Amsterdam, 1991), p. 139.
[5] W. M. Mueller, J. P. Blackledge, and G. G. Libowitz, *Metal Hydrides* (Academic Press, New York, 1968).
[6] H. D. Hochheimer, K. Strössner, W. Hönle, B. Baranowsky, and F. Filipek, Z. Phys. Chem., Neue Folge **143**, 139 (1985).
[7] S. J. Duclos, Y. K. Vohra, A. L. Ruoff, S. Filipek, and B. Baranowski, Phys. Rev. B **36**, 7664 (1987).
[8] K. Ghandehari, H. Luo, A. L. Ruoff, S. S. Trail, and F. J. Di Salvo, Phys. Rev. Lett. **74**, 2264 (1995).
[9] N. I. Kulikov, Fiz. Tverd. Tela (Leningrad) **20**, 2027 (1978) [Sov. Phys. Solid State **20**, 1170 (1978)].
[10] J. Hammerberg, J. Phys. Chem. Solids **39**, 617 (1978).
[11] J. L. Martins, Phys. Rev. B **41**, 7883 (1990).
[12] R. Ahuja, O. Eriksson, and B. Johansson, Physica B **265**, 87 (1999).
[13] A. M. Saitta, D. Alfe, S. de Gironcoli, and S. Baroni, Phys. Rev. Lett. **78**, 4958 (1997).
[14] S. Baroni, S. de Gironcoli, A. Corso, and P. Giannozzi, Rev. Mod. Phys. **73**, 515 (2001).
[15] K. Einarsdotter, B. Sadigh, G. Grimvall, and V. Ozoliņš, Phys. Rev. Lett. **79**, 2073 (1997).
[16] Y. Ma, J. S. Tse, and D. D. Klug, Phys. Rev. B **67**, 140301(R) (2003).
[17] Y. Ma, J. S. Tse, and D. D. Klug, Phys. Rev. B **69**, 064102 (2004).
[18] P. J. Craievich, M. Weinert, J. M. Sanchez, and R. E. Watson, Phys. Rev. Lett. **72**, 3076 (1994).
[19] P. J. Craievich, J. M. Sanchez, R. E. Watson, and M. Weinert, Phys. Rev. B **55**, 787 (1997).
[20] V. L. Sliwko, P. Mohn, K. Schwarz, and P. Blaha, J. Phys.: Condens. Matter **8**, 799 (1996).
[21] J. M. Wills, O. Eriksson, P. Söderlind, and A. M. Boring, Phys. Rev. Lett. **68**, 2802 (1992).
[22] S. Baroni, P. Giannozzi, and A. Testa, Phys. Rev. Lett. **58**, 1861 (1987).
[23] J. P. Perdew, and K. Burke, Int. J. Quantum Chem. **57**, 309 (1996); J. P. Perdew, K. Burke, and M. Ernzerhof, Phys. Rev. Lett. **77**, 3865 (1996).
[24] H. J. Monkhorst, and J. D. Pack, Phys. Rev. B **13**, 5188 (1976).
[25] P. Giannozzi, S. de Gironcoli, P. Pavone, and S. Baroni, Phys. Rev. B **43**, 7231 (1991).
[26] M. D. Segall, P. L. D. Lindan, M. J. Probert, C. J. Pickard, P. J. Hasnip, S. J. Clark, and M. C. Payne, J. Phys.: Condens. Matter **14**, 2717 (2002).
[27] F. D. Murnaghan, Proc. Natl. Acad. Sci. U.S.A. **30**, 244 (1944).
[28] L. Engebretsen (unpublished).
[29] C. O. Rodriguez and M. Methfessel, Phys. Rev. B **45**, 90 (1992).
[30] J. Hama, K. Suito, and N. Kawakami, Phys. Rev. B **39**, 3351 (1989).
[31] J. P. Vidal and G. Vidal-Valat, Acta Crystallogr., Sect. B: Struct. Sci. **42**, 131 (1986).
[32] D. Gerlich and C. S. Smith, J. Phys. Chem. Solids **35**, 1587 (1974).
[33] W. Pearson, P. Villars, and L. D. Calvere, *Pesrson's Handbook of Crystallographic Data for Intermetallic Phases* (ASM, Metals Park, Ohio, 1985).
[34] P. Loubeyre, R. L. Toullec, M. Hanfland, L. Ulivi, F. Datchi, and D. Hausermann, Phys. Rev. B **57**, 10403 (1998).
[35] G. Roma, C. M. Bertoni, and S. Baroni, Solid State Commun. **98**, 203 (1996).
[36] M. G. Zemlianov, E. G. Brovman, N. A. Chernoplekov, and Yu. L. Shitikov, *Inelastic Scattering of Neutrons* (IAEA, Vienna, 1965), Vol. II, p. 431.
[37] D. Laplaze, J. Phys. (France) **37**, 1051 (1976).
[38] G. Auffernann, G. D. Barrera, D. Colognesi, G. Corradi, A. J. Ramirez-Cuesta, and M. Zoppi, J. Phys.: Condens. Matter **16**, 5731 (2004).

[39] To carefully check the predicted phonon softening for NaH, KH, RbH, and CsH in RS structure, we also calculated the TA (X) phonon frequency with volume using another *ab initio* code of the ABINIT package (Ref. 50) within the implementation of linear response theory. In this tested calculation, we chose a kinetic energy cutoff of 70 Ry and a $8\times8\times8$ MP grid (k mesh) for all compounds. A phonon softening in TA (X) mode was also clearly revealed for these compounds. The predicted volumes for phonon softening to zero frequency using ABINIT are $0.43V_0$, $0.64V_0$, $0.74V_0$, and $0.82V_0$ for NaH, KH, RbH, and CsH, respectively, which in excellent agreement with the current calculations of $0.44V_0$, $0.61V_0$, $0.72V_0$, and $0.80V_0$. The small discrepancies in these two calculations are mainly due to the different choices of the pseudopotentials.

[40] A. D. B. Woods, B. N. Brochhouse, M. Sakamoto, and R. N. Senesi, *Inelastic Scattering in Liquids and Solids* (IAEA, Vienna, 1961), p. 487.

[41] R. S. Mulliken, J. Chem. Phys. **23**, 1833 (1955).

[42] M. D. Segall, R. Shah, C. J. Pickard, and M. C. Payne, Phys. Rev. B **54**, 16317 (1996).

[43] V. Ozoliņš and A. Zunger, Phys. Rev. Lett. **82**, 767 (1999).

[44] E. A. Ekimov, V. A. Sidorov, E. D. Bauer, N. N. Mel'nik, N. J. Curro, J. D. Thompson, and S. M. Stishov, Nature (London) **428**, 542 (2004).

[45] Y. Ma, J. S. Tse, T. Cui, D. D. Klug, L. Zhang, Y. Xie, Y. Niu, and G. Zou, Phys. Rev. B **72**, 014306 (2005).

[46] K. H. Hellwege and R. F. S. Hearmon, Vol. III of *Landolt-Börnstein*, New Series III (Springer, Berlin 1979).

[47] J. H. E. Jeffes and H. McKerrell, J. Iron Steel Inst., London **202**, 666 (1964).

[48] R. C. Bowman, J. Phys. Chem. **75**, 1251 (1971).

[49] V. I. Zinenko and A. S. Fedorov, Phys. Solid State **36**, 742 (1994).

[50] X. Gonze, J.-M. Beuken, R. Caracas, F. Detraux, M. Fuchs, G.-M. Rignanese, L. Sindic, M. Verstraete, G. Zerah, F. Jollet, M. torrent, A. Roy, M. Mikami, P. Ghosez, J.-Y. Raty, and D. C. Allan, Comput. Phys. Commun. **25**, 478 (2002).

[51] S. Baroni, A. Dal Corso, S. de Gironcoli, P. Giannozzi, C. Cavazzoni, G. Ballabio, S. Scandolo, G. Chiarotti, P. Focher, A. Pasquarello, K. Laasonen, A. Trave, R. Car, N. Marzari, and A. Kokalj, http://www.pwscf.org